Magnon-microwave backaction noise evasion in cavity magnomechanics

Bittencourt, Victor A.S.V.; Potts, C. A.; Davis, J. P.; Metelmann, A.

Important note
To cite this publication, please use the final published version (if applicable).
Please check the document version above.

Magnon-microwave backaction noise evasion in cavity magnomechanics

Victor A. S. V. Bittencourt [1] ✉, C. A. Potts [2,3,4], J. P. Davis [5] & A. Metelmann [1,6] ✉

In cavity magnomechanical systems, magnetic excitations couple simultaneously with mechanical vibrations and microwaves, incorporating the tunability of magnetism and the long lifetimes of mechanical modes. Applications of such systems, such as thermometry and sensing, require precise measurement of the mechanical degree-of-freedom with as less added noise as possible, a feature not proposed in the literature. In this paper, we propose a scheme for realizing backaction evading measurements of the mechanical vibrations in cavity magnomechanics. Our proposal involves driving the microwave cavity with two tones separated by twice the phonon frequency and with amplitudes satisfying a balance relation. We show that the minimum added imprecision noise is obtained for drives centered around the lower frequency magnon-microwave polaritons, which can beat the standard quantum limit at modest drive amplitudes. Our scheme is a simple and flexible way of engineering backaction evasion measurements that can be further generalized to other multimode systems.

One of the most iconic features of quantum mechanics is the disturbance of a system due to measurements[1]. The random nature of quantum measurements implies the addition of measurement noise to the system to be probed[2]. We can understand such a backaction effect by considering a simple quantum harmonic oscillator. Any position measurement will introduce a disturbance in the momentum, which is fed back to the position, manifesting itself as additional noise in future position measurements. Such measurement backaction effects can hinder applications that require precise measurement of an observable, in particular sensing.

Backaction evasion (BAE) schemes provide a pathway to evade any measurement backaction on an observable. This means that the measurement of such a quantum non-demolition (QND) observable does not disturb its evolution. The price to be paid is strong noise contamination in non-commuting observables. There are two requirements for a BAE scheme: the QND observable has to commute with itself at different times, and the QND observable has to commute with the interaction Hamiltonian describing the coupling between the measured system and the meter[1]. For a simple quantum harmonic oscillator, this can be accomplished, for instance, by measurements of the position quadrature as the QND observable, by means of a linear system-meter interaction Hamiltonian. System-meter interactions that yield BAE measurement can be engineered in hybrid systems architecture, a prominent example being the BAE scheme for measuring mechanical vibrations via light in optomechanical systems[3-8]. Other examples include electromechanical systems[9-12], atomic ensembles coupled to mechanical resonators[13], Bose-Einstein condensates[14], and superconducting qubits coupled to microwave cavities[15].

Cavity magnomechanical systems have recently emerged as a promising platform for quantum technologies[16,17]. In such systems, a magnetic element, usually made of yttrium iron garnet, is loaded into a microwave cavity, as we depict in Fig. 1. The magnetic excitations (magnons) couple simultaneously to the microwaves (via magnetic dipole coupling) and to the elastic vibrations of the material (via magnetoelastic effects)[16,18-20]. Typically, magnons and microwaves couple strongly and form hybrid magnon-microwave polaritons with frequencies defined by the coupling strength and the tunable magnon frequency. Such a system allows the drive and measurement of phonons via the microwave resonator while retaining the tunability of the magnons, as well as the use of the intrinsic magnon-microwave hybridization, for example, for efficient cooling and amplification of the mechanics[21]. Among the potential applications proposed for such systems are the generation of entangled states[22-24], the generation of squeezing of magnons and phonons via magnon nonlinearities[25,26], and noise-based thermometry[27]. The aforementioned applications require precise measurement of the mechanics and thus can be hindered by measurement backaction, an issue that has not been addressed in the field.

In this paper, we propose a BAE scheme for measuring phonon quadratures in a cavity magnomechanical system. Our scheme exploits the

[1]Institut de Science et d'Ingénierie Supramoléculaires (ISIS, UMR7006), Université de Strasbourg and CNRS, 67000 Strasbourg, France. [2]Kavli Institute of NanoScience, Delft University of Technology, PO Box 5046, 2600 GA Delft, Netherlands. [3]Niels Bohr Institute, University of Copenhagen, Blegdamsvej 17, 2100 Copenhagen, Denmark. [4]NNF Quantum Computing Programme, Niels Bohr Institute, University of Copenhagen, Copenhagen, Denmark. [5]Department of Physics, University of Alberta, Edmonton, AB, T6G 2E9, Canada. [6]Institute for Theory of Condensed Matter and Institute for Quantum Materials and Technology, Karlsruhe Institute of Technology, 76131 Karlsruhe, Germany. ✉e-mail: sant@unistra.fr; anja.metelmann@kit.edu
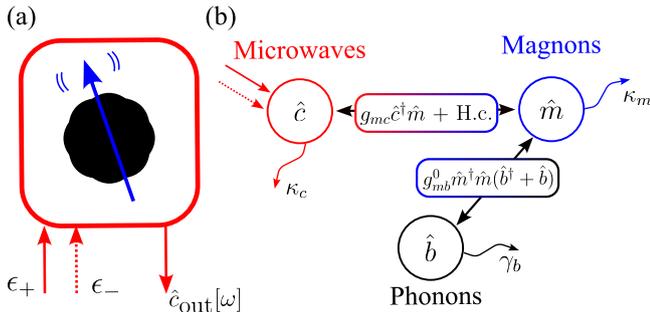
(a) (b)

Fig. 1 | Schematic depiction of a cavity magnomechanical system. a Schematic of the magnomechanical system for backaction evasion measurement of phonons: the magnetic excitations (blue) couple simultaneously to a microwave mode (red) and mechanical vibrations (black). The cavity is driven by two microwave tones ϵ and the output $\hat{c}_{\text{out}}$ is used to probe the mechanics. **b** The system is described by a model of interacting bosonic modes, $\hat{c}$ (microwave), $\hat{m}$ (magnon) and $\hat{b}$ (phonon) subject to dissipation with rates κ_c, κ_m and γ_b respectively. Magnons couple to microwaves with a rate g_{mc}, while the coupling to the phonon mode is via a parametric interaction with single-magnon coupling rate g_{mb}^0.

Table 1 | Typical parameters of a cavity magnomechanical system consisting of a magnetic sphere loaded in a 3D microwave cavity

Parameter	Symbol	Value
Microwave mode frequency	ω_c	$2\pi \times 10$ GHz
Magnon mode frequency	ω_m	ω_c
Phonon mode frequency	ω_b	$10^{-3}\omega_c$
Microwave total decay rate	κ_c	$2 \times 10^{-4}\omega_c$
Magnon mode decay rate	κ_m	$10^{-4}\omega_c$
Phonon intrinsic decay rate	γ_b	$10^{-7}\omega_c$
Magnon-microwave coupling rate	g_{mc}	$\sim 10^{-3}\omega_c$ (different cases will be considered)
Magnomechanical vacuum coupling rate	$g_{mb}^{(0)}$	$10^{-12}\omega_c$
Microwave drive amplitude	ϵ_d	in the range $\{10^3, 10^6\} \times \sqrt{\omega_c}$

radiation pressure-like coupling between the magnons and the mechanical mode to realize a QND Hamiltonian for a mechanical amplitude quadrature. The QND Hamiltonian is engineered by modulating the force driving the elastic vibrations due to magnetostriction, akin to BAE schemes proposed and implemented in opto and electromechanical systems[3,4,9]. Such modulation is accomplished by driving the microwave mode with two coherent tones, with balanced amplitudes. We then show that different hybrid mode separations yield different performances of the BAE scheme in terms of imprecision noise added to the mechanical measurement. At a reasonable drive amplitude, it is possible to beat the standard quantum limit of added noise. To study the robustness of the system we investigate in depth imperfections of the parameters. Our results present a simple yet robust framework for performing BAE measurements of mechanics in a cavity magnomechanical system, but they can be adapted to other multimode systems in which the measured system couples to a composite system exhibiting hybridization, for instance, optomechanical systems with two coupled optical cavities. Furthermore, the BAE scheme can be combined with other proposals, such as the use of nonlinearities for enhancing force measurements[28].

Results

Cavity magnomechanics and backaction noise

In this section, we introduce cavity magnomechanical systems and the effects of backaction noise on the measurement of the phonon mode in standard single-tone drive setups, which will provide a framework for the main core of our results.

The cavity magnomechanical system depicted in Fig. 1 can be modelled with the following Hamiltonian[16,20,29]

$$
\begin{aligned}
\frac{\hat{H}}{\hbar} =\ & \omega_c \hat{c}^\dagger \hat{c} + \omega_m \hat{m}^\dagger \hat{m} + \omega_b \hat{b}^\dagger \hat{b} + \frac{\hat{H}_{\text{drive}}}{\hbar} \\
& + g_{mc}\left(\hat{m}^\dagger \hat{c} + \hat{m}\hat{c}^\dagger\right) + g_{mb}^0 \hat{m}^\dagger \hat{m}\left(\hat{b}^\dagger + \hat{b}\right),
\end{aligned}
\tag{1}
$$

where $\hat{H}_{\text{drive}}$ denotes a coherent microwave drive term. A microwave mode $\hat{c}$ with frequency ω_c couples to a magnon mode $\hat{m}$ with frequency ω_m, which in turn couples to a phonon mode $\hat{b}$ with frequency ω_b. The magnon frequency ω_m can be tuned by an applied external field[30]. Magnons and microwaves couple via magnetic dipole interaction, which yields the coupling rate g_{mc}. At the same time, magnetoelastic effects[31] are responsible for coupling magnons and phonons with the single magnon coupling rate g_{mb}^0. We consider exclusively the coupling between the uniform magnon mode (the Kittel mode), with a single cavity mode and a single low-frequency phonon mode. We do not consider any direct coupling between phonons and microwaves, since such electromechanical coupling is typically not observable in magnomechanical experiments[16,21,32]. A more detailed discussion and derivation of the coupling rates can be found in Refs. 20,29. The numerical value of the parameters that we will use throughout the paper are summarized in Table 1 and correspond to experiments in which a 3D microwave cavity is loaded with a YIG sphere with radius $\sim 100\,\mu m$.

The microwave-magnon coupling can be stronger than both microwave and magnon decay rates, κ_c and κ_m respectively, generating a hybridization between the modes[33–35]. In such a regime, two polariton modes form at frequencies $\omega_\pm$. We call the mode with frequency $\omega_+ > \omega_-$ the upper hybrid mode while the other is the lower hybrid mode. In the case where the magnon mode is resonant with the microwave mode $\omega_m = \omega_c$, the difference between the hybrid modes frequencies is $\sim 2g_{mc}$. Throughout the paper, we will consider exclusively the situation in which magnons and microwaves are at resonance, corresponding to maximum hybridization between the modes.

The combination of the hybridization with the sidebands generated by the magnomechanical interaction gives a unique trait of the system in which the sidebands can lie close to the hybrid modes frequencies or overlap. This is depicted in Fig. 2 for the two configurations which we call triple resonance (modes split by one phonon frequency) and the dynamical backaction evasion schemes (modes split by twice phonon frequency), that have been explored in previous works[21,29,32]. These different configurations can be used for enhancing or balancing Stokes and anti-Stokes processes, yielding efficient cooling and amplification of the phonon mode[21], or dynamical backaction evasion[29,32]. These configurations can be tuned by changing the magnon-microwave coupling rate, which in turn depends on different parameters, such as the position of the sphere in the cavity, the volume of the cavity, and the volume of the sphere[34]. A change of g_{mc} in the range of $\omega_b/2$ is feasible in state-of-the-art systems via the above aforementioned parameters[27,34,36].

The measurement of the phonon mode can be accomplished by monitoring the output field of the microwave mode. Since the noise spectrum of the output field has imprints of the mechanical spectrum, the backaction noise driving the mechanics will unavoidably contaminate the measurement[2,5]. We describe this effect via the standard input-output relation for the microwave mode $\hat{c}_{\text{out}}[\omega] = \hat{c}_{\text{in}}[\omega] - \sqrt{\kappa_c}\hat{c}[\omega]$. The operator $\hat{c}[\omega]$ describes the fluctuations of the microwave cavity mode on top of a coherent state generated by the strong drive. It can be obtained by solving the linearized Heisenberg-Langevin equations in the frequency domain, which is shown in detail in Ref. 29 and in the Supplementary Notes 1. The main quantity of interest is the frequency-symmetrized noise spectrum of a
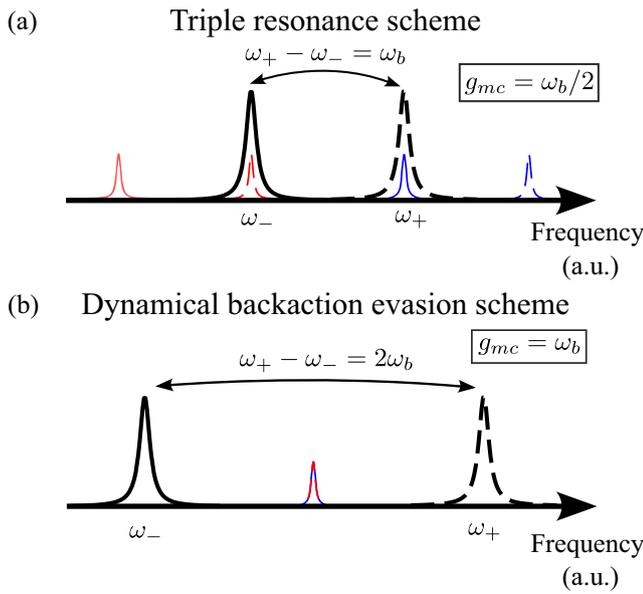
(a) Triple resonance scheme

(b) Dynamical backaction evasion scheme

Fig. 2 | Different cavity magnomechanics schemes. The Lorentzians indicate the resonance frequencies $\omega_\pm$ and linewidths of the hybrid modes as they would be measured, for example, via transmission. Relevant mechanical sidebands are also indicated. **a** Triple resonance scheme: the magnon-microwave coupling g_{mc} is half of the phonon frequency ω_b. The blue (red) sideband of the lower (upper) hybrid mode coincides with the upper (lower) hybrid mode frequency. **b** Dynamical backaction evasion scheme: the magnon-microwave coupling is equal to one phonon frequency. In this scheme, the sidebands of the hybrid modes coincide.

general quadrature

$$\hat{x}_{\theta,\text{out}}[\omega] = \frac{\hat{c}_{\text{out}}[\omega]e^{-i\theta} + \hat{c}^\dagger_{\text{out}}[\omega]e^{i\theta}}{\sqrt{2}}, \tag{2}$$

where θ is the quadrature angle, which is given by $\bar{S}_{\theta\theta}[\omega] = (S_{\theta\theta}[\omega] + S_{\theta\theta}[-\omega])/2$, where

$$S_{\theta\theta}[\omega] = \int_{-\infty}^{\infty} \frac{d\omega'}{2\pi} \langle \hat{x}_{\theta,\text{out}}[\omega], \hat{x}_{\theta,\text{out}}[\omega'] \rangle. \tag{3}$$

Typically, $\bar{S}_{\theta\theta}[\omega]$ is measured via a homodyne setup, where θ is tuned by a local field which is mixed with the output signal. The output noise spectrum yields

$$\bar{S}_{\theta\theta}[\omega] = |\mathcal{G}_\theta[\omega]|^2 \left[\bar{S}^{(0)}_{xx}[\omega] + \bar{S}_{\text{BA}}[\omega] + \bar{S}_{\text{imp}}[\omega] \right], \tag{4}$$

where $\bar{S}^{(0)}_{xx}[\omega]$, the uncoupled noise spectrum of the phonon mode, $|\mathcal{G}_\theta[\omega]|^2$ is the gain, which depends on the output quadrature being measured, $\bar{S}_{\text{BA}}[\omega]$ is the backaction noise contribution, stemming from the non-QND character of the quadrature being measured, and $\bar{S}_{\text{imp}}[\omega]$ is the imprecision noise, due to the unavoidable fluctuations in the input. We provide explicit expressions for all the terms appearing in Eq. (4) in the Supplementary Notes 2.

The goal of such a measurement is to probe $\bar{S}^{(0)}_{xx}[\omega]$, the uncoupled noise spectrum of the phonon mode, or mechanical noise spectrum, which is given by

$$\bar{S}^{(0)}_{xx}[\omega] = \frac{\gamma_b}{2}(2n_b + 1)\left(|\chi_b[\omega]|^2 + |\chi_b[-\omega]|^2\right), \tag{5}$$

where n_b is the phonon bath occupancy, and $\chi_b[\omega] = 1/(-i(\omega - \omega_b) + \gamma_b/2)$ is the phonon mode susceptibility. $\bar{S}^{(0)}_{xx}[\omega]$ has units of inverse frequency and

gives the position noise spectrum of the mechanical vibration via $x^2_{\text{ZPF}}\bar{S}^{(0)}_{xx}[\omega]$, where x_{ZPF} are the zero-point fluctuations of the phonon mode. For a magnomechanical system, x_{ZPF} depends on the elastic coefficients of the material as well as the particular mode profile of the elastic vibrations[29].

In addition to its thermal motion, the phonon mode experiences a displacement in response to the backaction noise. Such a displacement contaminates the measurement, manifesting as additional (backaction) noise added on top of the imprecision noise. In a typical optomechanical system with a single optical mode, the minimum added noise at the mechanical frequency, referred to as the standard quantum limit (SQL), is

$$\bar{S}^{\text{SQL}}_{\text{BA}}[\omega_b] + \bar{S}^{\text{SQL}}_{\text{imp}}[\omega_b] = \bar{S}^{(0)}_{xx}[\omega_b], \tag{6}$$

with the backaction and imprecision noise having equal contributions. Such minimum can be achieved by tuning the drive amplitude[5], which we indicate by ϵ_d. The SQL can also be written in terms of added quanta defined by

$$n_{\text{BA}} = \frac{\gamma_b}{4}\bar{S}_{\text{BA}}[\omega_b], \quad n_{\text{imp}} = \frac{\gamma_b}{4}\bar{S}_{\text{imp}}[\omega_b], \tag{7}$$

such that the total added quanta to the measurement is

$$n_{\text{add}} = n_{\text{BA}} + n_{\text{imp}}. \tag{8}$$

For a drive power achieving the SQL, we have

$$n^{\text{SQL}}_{\text{add}} = n^{\text{SQL}}_{\text{BA}} + n^{\text{SQL}}_{\text{imp}} = \frac{1}{2}. \tag{9}$$

In other words, in the best case, half a quanta is added to the measurement of the phonon mode. The imprecision noise is inversely proportional to the square of the drive amplitude, while the backaction noise grows with the same parameter. Such dependency can also be understood by recalling that the imprecision noise is related to the uncertainty on the measurement of a phase, which by itself satisfy a phase-number uncertainty relation[2]. This can be used to show that the imprecision noise is inversely proportional to the photon flux driving the cavity (proportional to $|\epsilon_d|^2$). Otherwise, the backaction noise depends directly on the mean number of magnons driven by the coherent tone, which is directly proportional to the input photon flux, and thus to $|\epsilon_d|^2$. The imprecision and backaction noise also satisfy an uncertainty-type relation, which implies such a behavior with the drive amplitude[2]. We give all the explicit formulas in the Supplementary Notes 2.

The hybridization between magnons and microwaves can prevent such a measurement from reaching the standard quantum limit, as the interplay between imprecision and backaction noise depends on the magnon-microwave coupling. This is shown in Fig. 3, which depicts the total added quanta to the measurement n_{add} as a function of the drive amplitude ϵ_d. The drive frequency ω_d is fixed at the magnon/microwave frequency $\omega_c = \omega_m$, since this choice eliminates dynamical backaction effects[29,32]. The interplay between the behavior of the imprecision and the backaction noise with the drive amplitude yields the minimum in Eq. (9) indicated by the dotted line in the figure. Since the measurement of the mechanics is performed via the microwaves instead of the directly coupled magnon mode, weaker magnon-microwave couplings yield smaller gains and, thus, larger imprecision noise, but also less backaction noise due to the smaller (linear) magnomechanical coupling. As a result, the minimum of the added noise for weaker magnon-microwave couplings is achieved at a higher drive amplitude than that for stronger magnon-microwave couplings.

Scheme for backaction noise evasion

In the last section, we have pointed out that the backaction noise driving the phonon mode is due to the non-QND nature of the position quadrature $\hat{x}_b$. To implement measurements that avoid backaction noise, we consider two requirements[1]: the observable to be measured has to commute with itself at
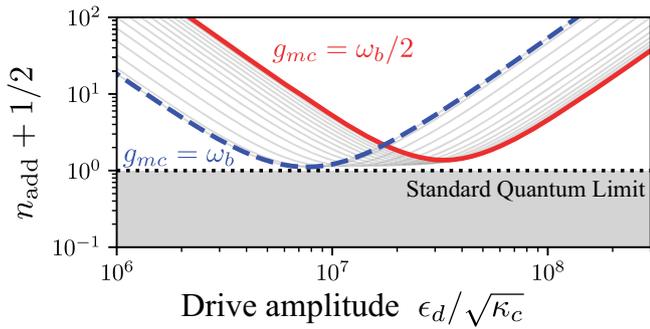
Fig. 3 | Number of added quanta to the measurement. The number of added quanta n_{add} is offset by the vacuum fluctuations in a single-tone cavity magnomechanical system at zero temperature and for a zero detuned drive as a function of the drive amplitude $\epsilon_d/\sqrt{\kappa_c}$, where κ_c is the microwave mode decay rate. The curves shown are for magnon-microwave couplings g_{mc} varying from $\omega_b/2$ (red, continuous curve) to ω_b (blue dashed line), with the thin lines corresponding to intermediate values. The values of drive amplitude depicted here correspond to linear magnomechanical couplings $|g_{mb}|$ in the range $\approx 10^{-3}\kappa_c$ to $0.5\kappa_c$. All other parameters as in Table 1.
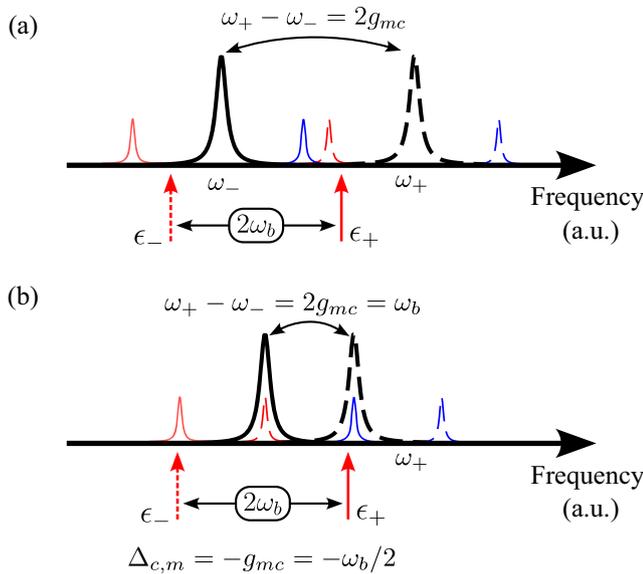

Fig. 4 | Frequency configuration for the backaction evasion scheme. a General framework: the two drive tones have to be separated by twice the phonon frequency ω_b, and the drive amplitudes $\epsilon_\pm$ have to satisfy Eq. (11). We have indicated the frequency of the lower frequency drive with a dashed arrow, and the higher frequency drive with a continuous arrow. The hybrid mode splitting $\omega_+ - \omega_- = 2g_{mc}$, where $\omega_\pm$ are the hybrid mode frequencies, can be arbitrary; **b** one particular configuration in which the mode splitting is set to the triple resonance scheme. In this case, the tones are centered around the lower hybrid mode. The high-frequency tone drives simultaneously the blue sideband of the lower hybrid mode and the upper hybrid mode. Such a configuration yields the minimum imprecision noise in the measurement of the backaction evading (BAE) quadrature via the microwave output.

all times, thus preventing the dynamics of the system from contaminating future measurements, and the measured observable has to commute with the system-meter interaction term, which ensures that no noise from the meter is fed into the system and then fed back to the measurement. This corresponds to a BAE measurement, which is also called a QND measurement.

To engineer a QND Hamiltonian for a quadrature of the phonon mode in a cavity magnomechanical system, we consider a two-tone microwave drive

$$\frac{\hat{H}_{drive}}{\hbar} = i\sqrt{\kappa_e}(\epsilon_- e^{-i\delta t} + \epsilon_+ e^{i\delta t})e^{i\omega_d t}\hat{c} + \text{H.c.},\tag{10}$$

in which the coherent tones $\pm$ have frequencies $\omega_d \pm \delta$, and phases $\nu_\pm$, i.e. $\epsilon_\pm = |\epsilon_\pm|e^{i\nu_\pm}$. To obtain a QND Hamiltonian, the drives should induce a modulation of the effective force $\propto \hat{m}^\dagger \hat{m}$ (see Eq. (1)) driving the phonon mode. This can be accomplished under two conditions: the frequency tone separation 2δ has to match twice the mechanical frequency $2\omega_b$, as shown in Fig. 4, and the drive amplitudes have to balance to guarantee that both drives yield the same (linear) magnomechanical coupling. The last requirement implies the following relation obtained which is obtained from the solution of the classical equations

$$\frac{|\epsilon_+|}{|\epsilon_-|} = \frac{\left|\left(i(\Delta_m + \omega_b) - \frac{\kappa_m}{2}\right)\left(i(\Delta_c + \omega_b) - \frac{\kappa_c}{2}\right) + g_{mc}^2\right|}{\left|\left(i(\Delta_m - \omega_b) - \frac{\kappa_m}{2}\right)\left(i(\Delta_c - \omega_b) - \frac{\kappa_c}{2}\right) + g_{mc}^2\right|},\tag{11}$$

in which $\Delta_{c,m} = \omega_d - \omega_{c,m}$ is the detuning between the central frequency of the drives ω_d and the magnon/microwave frequencies. More detailed calculations are provided in the Supplementary Notes 3. Such a strategy to engineer a BAE measurement of the mechanics is akin to the one proposed and implemented in opto and electromechanical system[3,4,9,10].

The two aforementioned conditions, the tones separation by twice the phonon frequency and the drive amplitudes balance in Eq. (11), engineer an effective modulation of the magnomechanical force driving the phonon mode. This in turn yield the linearized Hamiltonian of the system in the interacting frame with respect to $\omega_b \hat{b}^\dagger \hat{b}$ is

$$\frac{\hat{H}_{QND}}{\hbar} = -\frac{\Delta_c}{2}(\hat{x}_{c,\varphi}^2 + \hat{p}_{c,\varphi}^2) - \frac{\Delta_m}{2}(\hat{x}_{m,\varphi}^2 + \hat{p}_{m,\varphi}^2)$$
$$+ g_{mc}\left(\hat{x}_{m,\varphi}\hat{x}_{c,\varphi} + \hat{p}_{c,\varphi}\hat{p}_{m,\varphi}\right) + 2G\hat{x}_{m,\varphi}\hat{x}_{b,\psi}.\tag{12}$$

where the quadratures are defined as ($\alpha = c, m, b$)

$$\hat{x}_{\alpha,\phi} = \frac{e^{i\phi}\hat{\alpha}^\dagger + e^{-i\phi}\hat{\alpha}}{\sqrt{2}},$$
$$\hat{p}_{\alpha,\phi} = i\frac{e^{i\phi}\hat{\alpha}^\dagger - e^{-i\phi}\hat{\alpha}}{\sqrt{2}},\tag{13}$$

and the phases φ and ψ depend on the relative phases of the coherent steady-state of the magnon mode under the two-tone drive, whose amplitude defines the magnomechanical coupling G. This coupling rate depends linearly on the drive amplitude ϵ_+, and on the hybridization profile. The phases φ depend on the drive amplitudes phases $\nu_\pm$, on the central drive frequency (included in $\Delta_{m,c}$) and on the magnon-microwave hybridization profile. The explicit expressions for G, φ and ψ can be found in the Supplementary Notes 3. The Hamiltonian (12) is QND with respect to the phonon quadrature $\hat{x}_{b,\psi}$. By tuning the relative phase of the drive amplitudes, it is possible to change the phase ψ and thus to alter which phonon quadrature is QND. Such a quadrature is completely unaffected by the coupling to the magnons and by any measurement process done in the magnon-microwave part of the system. Nevertheless, due to the hybridization between magnons and microwaves, the quadrature $\hat{x}_{m,\varphi}$, through which one would measure $\hat{x}_{b,\psi}$ is not a QND observable. This is seen by analyzing the flowchart in Fig. 5, which illustrates the information flow in the system, for example, the magnon quadrature $\hat{p}_{m,\varphi}$ measures the phonon quadrature $\hat{x}_{b,\psi}$, passing the information to the quadratures $\hat{x}_{c,\varphi}$ and $\hat{x}_{m,\varphi}$. No quadrature feeds $\hat{x}_{b,\psi}$, since such a phonon quadrature is a QND observable. Otherwise, no magnon/microwave observable is QND. To note is, that the QND-nature of the mechanical quadrature $\hat{x}_{b,\psi}$ is as well preserved in the polariton basis.
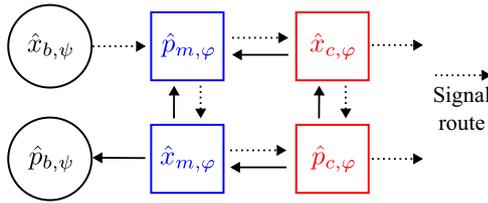
Fig. 5 | Flowchart schematizing the phonon signal's route in a magnomechanical system under the two-tones quantum non-demonilion (QND) scheme. The diagram represents the couplings between the quadratures $\hat{x}_{\alpha,\phi}$ and $\hat{p}_{\alpha,\phi}$ of the phonon (black), magnon (blue) and microwave (red) modes, in the QND Hamiltonian (12) (see Eq. (13)). The phases ψ and ϕ depend on the relative phases of the coherent magnon steady-state. We have indicated the route that the signal of the QND mechanical quadrature $\hat{x}_{b,\psi}$ takes with dotted arrows, while the black arrows indicate the route of the backaction noise that is dumped in $\hat{p}_{b,\psi}$. For a vanishing detuning $\Delta_c = 0$, the coupling between orthogonal magnon-microwave quadratures vanishes.

The solutions of the equations of motion for $\hat{x}_{b,\psi}$ and $\hat{p}_{b,\psi}$ in frequency domain are

$$\hat{x}_{b,\psi}[\omega] = \sqrt{\gamma_b}\hat{x}_{b,\psi,\text{in}}[\omega],$$
$$\hat{p}_{b,\psi}[\omega] = \sqrt{\gamma_b}\hat{p}_{b,\psi,\text{in}}[\omega] - 2G\chi_b[\omega]\hat{\xi}_{\text{BA},x_\varphi}[\omega] \qquad (14)$$
$$+ 2\sqrt{\gamma_b}\Sigma_b[\omega]\chi_b[\omega]\hat{x}_{b,\psi,\text{in}}[\omega].$$

The only term appearing in the equation for $\hat{x}_{b,\psi}[\omega]$ is the intrinsic (thermal and vacuum) noise driving the mechanics. Otherwise, all the backaction noise is dumped into the orthogonal quadrature $\hat{p}_{b,\psi}[\omega]$, which causes amplification of the noise of that quadrature. The noise terms $\hat{x}_{b,\psi,\text{in}}[\omega]$ and $\hat{p}_{b,\psi,\text{in}}[\omega]$ describe the intrinsic vacuum and thermal noise acting in the phonon mode, they have the correlations

$$\langle \hat{x}_{b,\psi,\text{in}}[\omega]\hat{x}_{b,\psi,\text{in}}[\omega'] \rangle = \langle \hat{p}_{b,\psi,\text{in}}[\omega]\hat{p}_{b,\psi,\text{in}}[\omega'] \rangle$$
$$= \pi\chi_b^2[\omega](2n_b + 1)\delta_{\text{D}}[\omega + \omega'],$$
$$\langle \hat{x}_{b,\psi,\text{in}}[\omega]\hat{p}_{b,\psi,\text{in}}[\omega'] \rangle = -\langle \hat{p}_{b,\psi,\text{in}}[\omega]\hat{x}_{b,\psi,\text{in}}[\omega'] \rangle \qquad (15)$$
$$= i\pi\chi_b^2[\omega]\delta_{\text{D}}[\omega + \omega'],$$

where $\delta_{\text{D}}[\omega + \omega']$ is the Dirac delta. In the equation for $\hat{p}_{b,\psi}$, $\Sigma_b[\omega]$ is called the phonon self-energy[27], given by

$$\Sigma_b[\omega] = iG^2\big(\Xi_m[\omega + \omega_b] - \Xi_m^*[-\omega - \omega_b]\big), \qquad (16)$$

where

$$\Xi_m^{-1}[\omega] = \chi_m^{-1}[\omega] + g_{mc}^2\chi_c[\omega]. \qquad (17)$$

is a modified magnon susceptibility. We have indicated the magnon and microwave susceptibilities by $\chi_{c,m}[\omega] = 1/(-i(\omega - \Delta_{m,c}) + \kappa_{m,c}/2)$. The backaction noise operator $\hat{\xi}_{\text{BA},x_\varphi}[\omega]$ has correlations

$$\langle \hat{\xi}_{\text{BA},x_\varphi}[\omega]\hat{\xi}_{\text{BA},x_\varphi}[\omega'] \rangle = \pi\Xi_m[\omega]\Xi_m^*[\omega']$$
$$\times (\kappa_m + g_{mc}\kappa_c\chi_c[\omega]\chi_c^*[\omega'])\delta_{\text{D}}[\omega + \omega'], \qquad (18)$$

where we have assumed that the magnon and microwave modes are at zero temperature.

Finally, unlike dynamical backaction evasion, the BAE scheme does not require the detunings to vanish. Nevertheless, to obtain Eq. (12), we have applied a rotating wave approximation (RWA) and discarded terms rotating at twice the phonon frequency. For the parameters considered here and at zero detuning, the corrections that the counter-rotating terms introduce in the integral of the phonon noise spectrum are $\sim 10^{-4}$ and can be safely

ignored, see the Supplementary Notes 4 and 5. At finite detunings, the analysis is more involved, but, since at all powers considered here the linearized magnomechanical coupling $|G| \ll \omega_b$, we expect that the RWA is a good approximation and thus that the same conclusions hold.

Microwave output spectrum and imprecision noise

We now turn our attention to the measurement of the QND quadrature via the output microwave signal. For this, we consider the standard input-output relation and compute the noise spectrum of a generalized output quadrature. In the present case, we can show that in a small bandwidth around zero frequency, the output noise spectrum is given by

$$\bar{S}_{\theta\theta}[\omega] = |\mathcal{G}_{x,\theta}[\omega]|^2 \left(\bar{S}_{xx}^{(0)}[\omega] + \frac{4n_{\text{imp},\theta}}{\gamma_b} \right), \qquad (19)$$

where $n_{\text{imp},\theta}$ is an effective number of quanta added to the measurement of the mechanical spectrum due to the imprecision noise. A detailed derivation of $\bar{S}_{\theta\theta}[\omega]$ is given in the Supplementary Notes 7. Since the scheme is BAE, there is no noise added by backaction, compared with Eq. (4).

The imprecision noise depends on the ratio between the uncoupled output spectrum and the gain factor evaluated at zero frequency

$$n_{\text{imp},\theta} \propto \frac{\bar{S}_{\text{out}}^{(0)}[0]}{|\mathcal{G}_{x,\theta}[0]|^2}, \qquad (20)$$

where $\bar{S}_{\text{out}}^{(0)}[0]$ is the output spectrum in the absence of the magnomechanical coupling, which exhibits two minima for drives centered around the hybrid modes frequencies $\omega_\pm = \omega_c \pm g_{mc}$. In conjunction with a minimal $\bar{S}_{\text{out}}^{(0)}[0]$, the impression noise is suppressed at large gain, which can be achieved at optimized detunings. However, the gain factor for arbitrary detuning can be written as

$$|\mathcal{G}_{x,\theta}[0]|^2 = 2\kappa_c|G|^2g_{mc}^2 \left(\frac{1}{|\lambda_+|^2|\lambda_-|^2} + 2\text{Re}\left[\frac{e^{2i(\varphi-\theta)}}{\lambda_+^2\lambda_-^2} \right] \right), \qquad (21)$$

where $\lambda_\pm = i(\omega_d - \omega_\pm) - (\kappa_c + \kappa_m)/4$. This gain factor is maximized for drives centered around the hybrid modes $\omega_d = \omega_\pm$, or, correspondingly, a detuning $\Delta_c = \mp g_{mc}$. In these cases

$$n_{\text{imp},\theta} = \frac{\gamma_b}{4}\frac{\kappa_{\text{eqv},\theta}}{32G^2}. \qquad (22)$$

In this form, the imprecision noise has the same expression as for a single-cavity optomechanical system[3], with an equivalent decay $\kappa_{\text{eqv},\theta}$ given by

$$\kappa_{\text{eqv},\theta} = \frac{\left(g_{mc}^2(\kappa_c + \kappa_m)^2 + \frac{\kappa_c^2\kappa_m^2}{4} \right)^2}{\kappa_c g_{mc}^2 \left(\frac{\kappa_m\kappa_m}{4}\cos(\varphi - \theta) \pm g_{mc}\kappa_\pm \sin(\varphi - \theta) \right)^2}. \qquad (23)$$

The output measurement angle θ_{opt} that minimizes the above expression is

$$\tan(\varphi - \theta_{\text{opt}}) = \pm\frac{4g_{mc}(\kappa_c + \kappa_m)}{\kappa_c\kappa_m}. \qquad (24)$$

The quadrature that optimizes the measurement gain depends on the magnon-microwave coupling and the decay rates, and it is, therefore, related to the hybridization. In fact, by inspecting the flowchart in Fig. 5, we notice that the signal of the mechanical quadrature distributes among the microwave quadratures due to the coupling between microwave and magnons. For the optimum measurement quadrature, the minimum added quanta
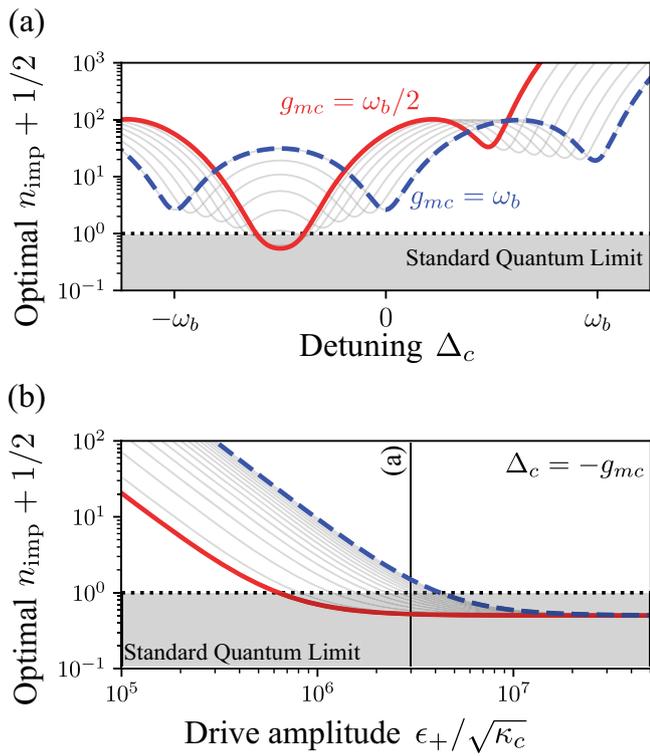
(a)

$g_{mc} = \omega_b/2$

$g_{mc} = \omega_b$

Standard Quantum Limit

Detuning Δ_c

(b)

(a)

$\Delta_c = -g_{mc}$

Standard Quantum Limit

Drive amplitude $\epsilon_+/\sqrt{\kappa_c}$

Fig. 6 | Number of added quanta due to imprecision noise for the optimal output quadrature. a Number of imprecision quanta n_{imp} as a function of the cavity-drive detuning Δ_c and (**b**) as a function of the drive amplitude ϵ_+. Plots for magnon-microwave couplings ranging from $\omega_b/2$ (red curve) to ω_b (blue-dashed curve), where ω_b is the phonon frequency. In (**a**), we set the drive amplitude $\epsilon_+/\sqrt{\kappa_c} = 2 \times 10^6$. The gray curves correspond to intermediate values of the magnon-microwave coupling g_{mc}. The dotted line indicates the standard quantum limit (SQL) for added noise $n_{\mathrm{imp}}^{\mathrm{SQL}} = 1/2$. Plot for zero temperature and all parameters as in Table 1. The coupling rate G scales linearly with ϵ_+, being in the range from $\sim 10^{-5}\omega_b$ (for $g_{mc} = \omega_b$ at the lowest powers) to $\sim 10^{-1}\omega_b$ (for $g_{mc} = \omega_b/2$ at the highest powers). κ_c indicates the microwave mode decay rate.

added to the measurement is

$$n_{\mathrm{imp,opt}} = \frac{\gamma_b}{32G^2 g_{mc}^2 \kappa_c}\left(g_{mc}^2 \frac{(\kappa_c + \kappa_m)^2}{4} + \frac{\kappa_c^2 \kappa_m^2}{16}\right). \quad (25)$$

The corresponding equivalent decay $\kappa_{\mathrm{imp,opt}}$ is always larger than both κ_c and κ_m.

To assess the performance of our BAE scheme under different configurations of the system, we first evaluate how the imprecision noise behaves for different magnon-microwave mode splittings. Furthermore, we consider real drive amplitudes $\epsilon_\pm$ in Eq. (10), since the drive phases will only change the QND quadrature and the optimal output quadrature to be measured. In Fig. 6a, we show the optimal added quanta (offset by the vacuum fluctuations 1/2) as a function of the detuning to the central frequency of the drives $\Delta_c = \Delta_m$ for magnon-microwave couplings ranging from $\omega_b/2$ (triple resonance) to ω_b (dynamical backaction evasion). We observe in the curve the predicted minima of the added noise for detunings at the frequencies of the hybrid modes. The global minimum of added imprecision noise is obtained in the triple resonance scheme for a detuning set at the lower hybrid mode. In this case, the high-frequency tone is at the higher hybrid mode, while the lower-frequency tone is at the red mechanical sideband of the lower hybrid mode. The imprecision noise n_{imp} can be made arbitrarily small by increasing the driving amplitude. In such a perfect scenario, the added quanta to the measurement can go below the SQL, $n_{\mathrm{imp}}^{\mathrm{SQL}} = 1/2$. We show the scaling of the added quanta (offset by the vacuum noise) as a function of power for tones centered around the lower hybrid
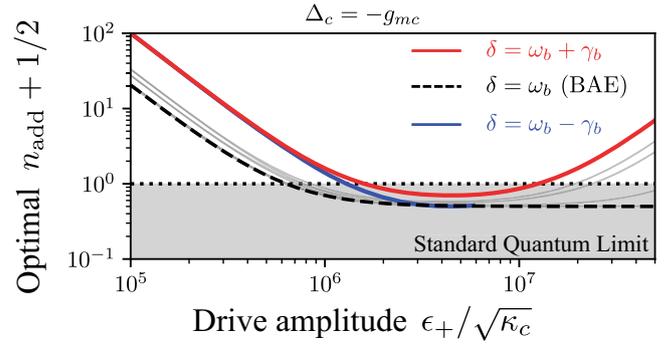
Fig. 7 | Added quanta to the measurement of the phonon mode for imperfect tone separation. The total amount of added quanta n_{add} (offset by the vacuum noise 1/2) is shown as a function of the drive amplitude ϵ_+ for several values of half of the tones frequency difference δ ranging from $\omega_b - \gamma_b$ (blue curve) to $\omega_b + \gamma_b$ (red curve), where ω_b is the phonon frequency and γ_b the phonon decay rate. The magnon-microwave coupling g_{mc} is fixed at $\omega_b/2$ (triple resonance scheme), and the drives are centered around the lower hybrid mode $\Delta_c = -g_{mc}$, where Δ_c is the detuning to the microwave frequency. The curve corresponding to the backaction evading (BAE) scheme is indicated by a dashed line and the standard quantum limit (SQL) by a dotted line. κ_c is the microwave decay rate and all parameters are given in Table 1.

mode in Fig. 6b. In contrast with the single-tone case, shown in Fig. 3, the added noise in the BAE scheme decreases with the drive amplitude since the only source of added noise is the imprecision noise. Stronger magnon-microwave couplings require a stronger drive to beat the SQL, as we can see by comparing the results of the triple resonance configuration (continuous line) with the one for the dynamical backaction evasion configuration (dashed lines). We also notice that in the BAE scheme, it is possible to achieve a more precise measurement of the mechanics (less added noise) at weaker drive amplitudes in comparison with a single-tone drive.

The analysis performed above relies on an RWA, which holds in the 'good cavity' regime $\kappa_{c,m} < \omega_b$ and for weak magnomechanical couplings. In fact, for the results in Fig. 3, the maximum value of the linear magnomechanical coupling rate is $G \sim 10^{-1}\omega_b$, for which the RWA should be still valid to a good approximation. Otherwise, we notice that, for the parameters in Fig. 3b the considered configurations beat the SQL at a coupling strength $G \sim 10^{-2}\omega_b$. Analogously to standard optomechanical system[3], we expect that our scheme can cope with corrections introduced by the RWA and still beat the quantum limit. The added noise also depends on the magnon/microwave bath occupancy and on the drive power, see the Supplementary Notes 8 for explicit expressions. For the parameters we considered here, the scheme is able to beat the SQL for magnon/microwave bath occupancies up to a few hundred quanta. For magnon/microwave modes with ~ 10 GHz frequencies, a negligible occupancy can be attained at a few hundreds of mK, which is routinely achieved in cavity magnonic experiments[33,37].

Robustness of the backaction evasion scheme under imperfect tones separation

There are two requirements for BAE: the two tones applied to the microwave have to be separated by $2\delta = 2\omega_b$, and the amplitude of the tones has to be such that Eq. (11) is satisfied. Nevertheless, it might be hard to achieve such requirements perfectly in practical setups. We consider here the effects of an imperfect tones separation in the added noise to the phonon measurement.

Deviations from the requirements for BAE change the measured phonon noise spectrum, adding backaction noise. The form of the measured output spectrum, in this case, resembles the one given in Eq. (3), but with a modified backaction noise term, whose effect depends on both the mode splitting and the central tones frequency. We consider first the optimum point of the imprecision noise shown in Fig. 6a, obtained for the triple resonance scheme and a central frequency with detuning $\Delta_c = -g_{mc}$. We show in Fig. 7 the total added noise (imprecision plus backaction contributions) for different values of the tones
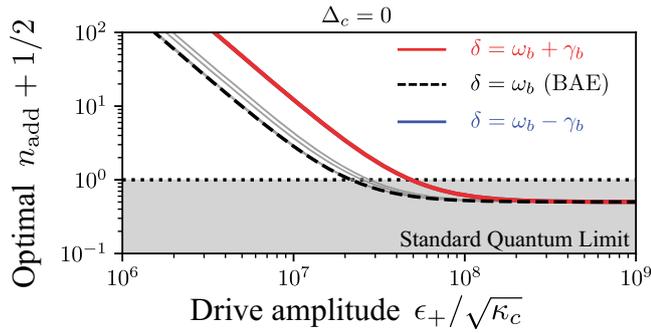
Fig. 8 | Added quanta to the measurement of the phonon mode for imperfect tone separation and zero detuning. The total amount of added quanta n_{add} (offset by the vacuum noise 1/2) is shown as a function of the drive amplitude ϵ_+ for several values of half of the tones frequency difference δ ranging from $\omega_b - \gamma_b$ (blue curve) to $\omega_b + \gamma_b$ (red curve), where ω_b is the phonon frequency and γ_b the phonon decay rate. The magnon-microwave coupling g_{mc} is fixed at $\omega_b/2$ (triple resonance scheme), and the drives are centered around the cavity/magnon frequency $\Delta_c = 0$. The curve corresponding to the backaction evading (BAE) scheme is indicated by a dashed line and the standard quantum limit (SQL) by a dotted line. The blue line coincides with the red line. κ_c is the microwave mode decay rate and all parameters are given in Table 1.

frequency difference δ. As the tone separation deviates from the BAE value, the added noise curve starts to become deformed at higher powers due to the backaction noise contribution. The imprecision noise contribution is also modified, getting stronger; nevertheless, we notice that even under such imperfect parameters, the measurement with a double tone can still beat the SQL at weaker drive amplitudes when compared with the single tone setup, compare with Fig. 6. For tones separation $< 2\omega_b$, there is a drive amplitude range in which the measured phonon noise goes below the reference BAE value as a consequence of backaction squeezing of the mechanics and enhancement of the measurement gain. Correspondingly, the orthogonal quadrature is amplified. The system can also enter unstable regimes, at which the curves are abruptly ended. Similar results to those shown in Fig. 7 are obtained in other cases, for instance, for imperfect drive amplitude balances, in correspondence with observations in electromechanical systems[10], and in agreement with recent proposals for generating microwave squeezing[38,39].

We can compare the robustness of the BAE scheme under a different choice parameters. As an example, we keep the hybrid mode splitting fixed, e.g. $g_{mc} = \omega_b/2$, and consider a different choice of the detuning $\Delta_c = 0$. The total added noise for this case is shown in Fig. 8. Even though this choice requires a stronger power to beat the SQL, we notice that there are no instabilities for the same range of added noise, and that, for the powers depicted here, the added noise curves show no apparent deformation due to backaction noise. Such facts suggest that this scheme is more robust to imperfect tone separation, even though it does not provides the minimum of imprecision noise at a given drive power in the perfect BAE scheme. There is thus an interplay between robustness and optimum added noise to the measurement of the phonon mode that has to be considered for experimental implementations.

Finally, results for imperfect drive amplitude balance exhibit a similar behavior to the ones shown here, pointing to the same conclusion about the interplay between robustness and minimum added noise.

Conclusion

To summarize, we have proposed and characterized a scheme for backaction evasion measurement of a mechanical quadrature tailored for cavity magnomechanical systems. Different schemes for backaction evasion are possible, and we have studied their robustness to imperfections of the BAE requirements, as well as the amount of noise added to the measurement via the output of the microwave mode. We have show that, at a given driven power, the minimum imprecision noise can be

obtained for a system in triple resonance with drives centered around the lower frequency hybrid mode. In fact, in this case, state-of-the-art systems can go below the standard quantum limit at dilution fridge temperatures. Nevertheless, such a scheme is not the more robust to imperfections, exhibiting significant deviations from the BAE case which are less prominent in other configurations.

Our results provide a simple and flexible route for measuring phonons in cavity magnomechanics. For instance, such a quantum backaction evasion scheme can be used to perform quantum tomography of phonons and validate the creation of entangled and squeezed states proposed in the literature. A more complete model should include imperfect measurement efficiency as well as other intrinsic features of cavity magnomechanical systems, in particular, magnetic nonlinearities and the unavoidable coupling to high-order Walker modes and to multiple phonon modes[29]. We should notice that, for a magnetic sphere, if the microwave mode is uniform at the sphere's position, the only the Kittel mode couples to the microwave[34]. Otherwise, in experiments such as[16,21,32], all the aforementioned contributions are small and can be discarded at weak drive amplitudes. We present a brief analysis of this point in the Supplementary Notes 9, and a more complete analysis is postponed to a future work.

Methods

Output spectrum and number of added quanta for single tone cavity magnomechanics

To obtain the results shown in Fig. 3, one proceeds as follows. Starting from the cavity magnomechanics Hamiltonian (1) with the drive term $\hat{H}_{drive} = \hbar i \sqrt{\kappa_e} \epsilon_d (\hat{c} e^{i\omega_d t} - \hat{c}^\dagger e^{-i\omega_d t})$, we move to a rotating frame with the drive frequency ω_d and obtain a set of non-linear Heisenberg-Langevin equations for the operators $\hat{c}$, $\hat{m}$ and $\hat{b}$. By taking the expectation values of the equations and using a mean-field approximation, we obtain the semi-classical steady-state solutions $\bar{\alpha}$ ($\alpha = c, m, b$). We then linearize the Hamiltonian (1) by writing the annihilation operators as $\hat{\alpha} = \bar{\alpha} + \delta\hat{\alpha}$. The Hamiltonian Eq. (1) is then truncated up to second order on the fluctuations operators $\delta\hat{\alpha}$. From simplicity, we drop the δ indicating the fluctuations. The linearized magnomechanical Hamiltonian, in the frame rotating with the laser frequency ω_d is thus given by

$$\frac{\hat{H}}{\hbar} = \omega_b \hat{b}^\dagger \hat{b} + g_{mc}(\hat{m}^\dagger \hat{c} + \hat{c}^\dagger \hat{m})$$
$$+ i|g_{mb}|(\hat{m}^\dagger - \hat{m})(\hat{b}^\dagger + \hat{b}), \tag{26}$$

where $g_{mb} = \bar{m} g_{mb}^0$ is the linear magnomechanical coupling. Such a linearization procedure is standard and more details can be found, for example, in[21].

To obtain the output spectrum, we first solve the linear dynamics of the system, given by the Heisenberg-Langevin equations

$$\partial_t \hat{\alpha} = \frac{i}{\hbar}[\hat{H}, \hat{\alpha}] - \frac{\kappa_\alpha}{2}\hat{\alpha} + \sqrt{\kappa_\alpha}\hat{\alpha}_{in}(t), \tag{27}$$

for $\alpha = c, m, b$. The noise terms are thermal and vacuum noises with correlations given by

$$\langle \hat{\alpha}_{in}(t)\hat{\alpha}_{in}^\dagger(t') \rangle = (n_\alpha + 1)\delta(t - t'),$$
$$\langle \hat{\alpha}_{in}^\dagger(t)\hat{\alpha}_{in}(t') \rangle = n_\alpha \delta(t - t'), \tag{28}$$

where n_α is the α mode bath occupancy. For magnons and microwaves we set $n_{c,m} = 0$.

The obtained linear set of equations in time domain is then transformed to frequency domain by standard Fourier transformation. The linear set of equations is solved for $\hat{c}[\omega]$, the annihilation operator of the microwave mode in frequency domain, in terms of the noise operators

whose correlations in can be obtained from Eq. (28) as

$$
\begin{aligned}
\langle \hat{\alpha}_{\text{in}}[\omega]\hat{\alpha}_{\text{in}}^{\dagger}[\omega']\rangle &= 2\pi(n_\alpha + 1)\delta(\omega + \omega'), \\
\langle \hat{\alpha}_{\text{in}}^{\dagger}[\omega]\hat{\alpha}_{\text{in}}[\omega']\rangle &= 2\pi n_\alpha \delta(\omega + \omega').
\end{aligned}
\tag{29}
$$

We then use the input-output relation $\hat{c}_{\text{out}}[\omega] = \hat{c}_{\text{in}}[\omega] - \sqrt{\kappa_c}\hat{c}[\omega]$, to obtain $\hat{c}_{\text{out}}[\omega]$ in terms of all the input noises, from where we can construct the output quadrature $\hat{x}_{\theta,\text{out}}[\omega]$ given in Eq. (2). The noise correlations in Eqs. (29) can then be used to compute the noise spectrum $S_{\theta\theta}[\omega]$ of Eq. (3), from where the signal, backaction and imprecision noise contribution can be identified. This is also the quantity we use to defined the added quanta to the measurement presented in the Results section. More detailed calculations are given in the Supplementary Notes 1 and 2.

Output spectrum and number of added quanta for the two-tone backaction evasion scheme

To obtain the QND Hamiltonian in Eq. (12) and the corresponding microwave output spectrum, we proceed as follows.

We start from the magnomechanical Hamiltonian (1) with the two-tone drive term $\hat{H}_{\text{drive}} = \hbar i \sqrt{\kappa_e}(\epsilon_- e^{-i\delta t} + \epsilon_+ e^{i\delta t})e^{i\omega_d t}\hat{c} + \text{H.c.}$, and move to a rotating frame with frequency ω_d. We then make the ansatz $\hat{c} = \hat{c}_0 + \hat{c}_+ e^{-i\delta t} + \hat{c}_- e^{i\delta t}$ and $\hat{m} = \hat{m}_0 + \hat{m}_+ e^{-i\delta t} + \hat{m}_- e^{i\delta t}$, and obtain from the Heisenberg-Langevin equations, a set of nonlinear coupled equations for the expectation values of the annihilation operators. Similar to the previous case, we use those to obtain steady-state coherent solutions, which we use to linearize the Hamiltonian by $\hat{\alpha} = \delta\hat{\alpha} + \bar{\alpha}_+ e^{-i\delta t} + \bar{\alpha}_- e^{i\delta t}$ for $\alpha = c, m$ and, again, discarding any contributions that involve products of more than two fluctuation operators.

In the interacting frame with $\omega_b \hat{b}^{\dagger}\hat{b}$, the linearized Hamiltonian reads

$$
\begin{aligned}
\frac{\hat{H}_L^{(2)}}{\hbar} =& -\Delta_c \hat{c}^{\dagger}\hat{c} - \Delta_m \hat{m}^{\dagger}\hat{m} + g_{mc}\left(\hat{m}^{\dagger}\hat{c} + \hat{m}\hat{c}^{\dagger}\right) \\
&+ e^{i\delta t}\left(g_- \hat{m}^{\dagger} + g_+^* \hat{m}\right)\left(\hat{b}e^{-i\omega_b t} + \hat{b}^{\dagger}e^{i\omega_b t}\right) \\
&+ e^{-i\delta t}\left(g_+ \hat{m}^{\dagger} + g_-^* \hat{m}\right)\left(\hat{b}e^{-i\omega_b t} + \hat{b}^{\dagger}e^{i\omega_b t}\right),
\end{aligned}
\tag{30}
$$

where we have defined $g_{\pm} = g_{mb}^0 \bar{m}_{\pm}$. Under the conditions for backaction evasion, we have $|g_+| = |g_-|$, and we can perform a RWA to discard any terms proportional to $e^{\pm 2i\omega_b}$. Such procedure yields the QND Hamiltonian of Eq. (12).

From the QND Hamiltonian, we obtain the set of linear Heisenberg-Langevin equations for the annihilation operators of the fluctuations, which, similar to the previous case, we can solve in frequency domain. We solve for $\hat{c}[\omega]$, which is the used with the input-output relation to obtain $\hat{c}_{\text{out}}[\omega]$. Finally, the output operator can be used to calculate the output noise spectrum which, in this case, has only the phonon signal and the imprecision noise contributions. The latter can be used to defined the added quanta given in Eq. (20), which is plotted in Fig. 6. Full derivations are presented in the Supplementary Notes 3–7, which also include an evaluation of the RWA.

The results under imperfect conditions are obtained following the same procedure, as outlined in the Supplementary Notes 8.

Data availability
All the plots of this paper were generated with the analytical expressions derived using standard Python plotting libraries.

Code availability
Codes for generating the plots can be provided upon reasonable request.

References
1. Braginsky, V. B., Vorontsov, Y. I. & Thorne, K. S. Quantum nondemolition measurements. *Science* **209**, 547–557 (1980).
2. Clerk, A. A., Devoret, M. H., Girvin, S. M., Marquardt, F. & Schoelkopf, R. J. Introduction to quantum noise, measurement, and amplification. *Rev. Mod. Phys.* **82**, 1155–1208 (2010).
3. Clerk, A. A., Marquardt, F. & Jacobs, K. Back-action evasion and squeezing of a mechanical resonator using a cavity detector. *New J. Phys.* **10**, 095010 (2008).
4. Woolley, M. J. & Clerk, A. A. Two-mode back-action-evading measurements in cavity optomechanics. *Phys. Rev. A* **87**, 063846 (2013).
5. Aspelmeyer, M., Kippenberg, T. J. & Marquardt, F. Cavity optomechanics. *Rev. Mod. Phys.* **86**, 1391 (2014).
6. Yanay, Y. & Clerk, A. A. Shelving-style qnd phonon-number detection in quantum optomechanics. *New J. Phys.* **19**, 033014 (2017).
7. Hauer, B. D., Metelmann, A. & Davis, J. P. Phonon quantum nondemolition measurements in nonlinearly coupled optomechanical cavities. *Phys. Rev. A* **98**, 043804 (2018).
8. Shomroni, I., Qiu, L., Malz, D., Nunnenkamp, A. & Kippenberg, T. J. Optical backaction-evading measurement of a mechanical oscillator. *Nat. Commun.* **10**, 1–7 (2019).
9. Hertzberg, J. et al. Back-action-evading measurements of nanomechanical motion. *Nat. Phys.* **6**, 213–217 (2010).
10. Lecocq, F., Clark, J. B., Simmonds, R. W., Aumentado, J. & Teufel, J. D. Quantum nondemolition measurement of a nonclassical state of a massive object. *Phys. Rev. X* **5**, 041037 (2015).
11. Ockeloen-Korppi, C. et al. Quantum backaction evading measurement of collective mechanical modes. *Phys. Rev. Lett.* **117**, 140401 (2016).
12. Liu, Y., Zhou, J., de Lépinay, L. M. & Sillanpää, M. A. Quantum backaction evading measurements of a silicon nitride membrane resonator. *New J. Phys.* **24**, 083043 (2022).
13. Møller, C. B. et al. Quantum back-action-evading measurement of motion in a negative mass reference frame. *Nature* **547**, 191–195 (2017).
14. Altuntaş, E. & Spielman, I. B. Quantum back-action limits in dispersively measured bose-einstein condensates. *Commun. Phys.* **6**, 66 (2023).
15. Gambetta, J. et al. Qubit-photon interactions in a cavity: Measurement-induced dephasing and number splitting. *Phys. Rev. A* **74**, 042318 (2006).
16. Zhang, X., Zou, C.-L., Jiang, L. & Tang, H. X. Cavity magnomechanics. *Sci. Adv.* **2**, e1501286 (2016).
17. Rameshti, B. Z. et al. Cavity magnonics. *Phys. Rep.* **979**, 1–61 (2022).
18. LeCraw, R., Spencer, E. & Gordon, E. Extremely low loss acoustic resonance in single-crystal garnet spheres. *Phys. Rev. Lett.* **6**, 620 (1961).
19. Spencer, E. G. & LeCraw, R. Magnetoacoustic resonance in yttrium iron garnet. *Phys. Rev. Lett.* **1**, 241 (1958).
20. Gonzalez-Ballestero, C., Hümmer, D., Gieseler, J. & Romero-Isart, O. Theory of quantum acoustomagnonics and acoustomechanics with a micromagnet. *Phys. Rev. B* **101**, 125404 (2020).
21. Potts, C. A., Varga, E., Bittencourt, V. A. S. V., Viola Kusminskiy, S. & Davis, J. P. Dynamical backaction magnomechanics. *Phys. Rev. X* **11**, 031053 (2021).
22. Li, J., Zhu, S.-Y. & Agarwal, G. Magnon-photon-phonon entanglement in cavity magnomechanics. *Phys. Rev. Lett.* **121**, 203601 (2018).
23. Li, J. & Gröblacher, S. Entangling the vibrational modes of two massive ferromagnetic spheres using cavity magnomechanics. *Quantum Sci. Technol.* **6**, 024005 (2021).

24. Fan, Z.-Y., Qiu, L., Gröblacher, S. & Li, J. Microwave-optics entanglement via cavity optomagnomechanics. *Laser Photonics Rev.* **n/a**, 2200866 (2022).

25. Li, J., Wang, Y.-P., You, J.-Q. & Zhu, S.-Y. Squeezing microwaves by magnetostriction. *Nat. Sci. Rev.* **10**, nwac247 (2022).

26. Ding, M.-S., Zheng, L., Shi, Y. & Liu, Y.-J. Magnon squeezing enhanced entanglement in a cavity magnomechanical system. *J. Opt. Soc. Am. B* **39**, 2665–2669 (2022).

27. Potts, C. A., Bittencourt, V. A. S. V., Viola Kusminskiy, S. & Davis, J. P. Magnon-phonon quantum correlation thermometry. *Phys. Rev. Appl.* **13**, 064001 (2020).

28. Zhang, Q. et al. Quantum weak force sensing with squeezed magnomechanics. *Sci. China Physics, Mech. Astronomy* **67**, 100313 (2024).

29. Bittencourt, V. A. S. V., Potts, C. A., Huang, Y., Davis, J. P. & Viola Kusminskiy, S. Magnomechanical backaction corrections due to coupling to higher-order walker modes and kerr nonlinearities. *Phys. Rev. B* **107**, 144411 (2023).

30. Stancil, D. D. & Prabhakar, A. *Spin Waves: Theory and Applications* (Springer, New York, 2010).

31. Callen, E. Magnetostriction. *J. Appl. Phys.* **39**, 519–527 (1968).

32. Potts, C. A., Huang, Y., Bittencourt, V. A. S. V., Viola Kusminskiy, S. & Davis, J. P. Dynamical backaction evading magnomechanics. *Phys. Rev. B* **107**, L140405 (2023).

33. Huebl, H. et al. High cooperativity in coupled microwave resonator ferrimagnetic insulator hybrids. *Phys. Rev. Lett.* **111**, 127003 (2013).

34. Zhang, X., Zou, C.-L., Jiang, L. & Tang, H. X. Strongly coupled magnons and cavity microwave photons. *Phys. Rev. Lett.* **113**, 156401 (2014).

35. Potts, C. A. & Davis, J. P. Strong magnon–photon coupling within a tunable cryogenic microwave cavity. *Appl. Phys. Lett.* **116**, 263503 (2020).

36. Zhang, X., Ding, K., Zhou, X., Xu, J. & Jin, D. Experimental observation of an exceptional surface in synthetic dimensions with magnon polaritons. *Phys. Rev. Lett.* **123**, 237202 (2019).

37. Lachance-Quirion, D., Tabuchi, Y., Gloppe, A., Usami, K. & Nakamura, Y. Hybrid quantum systems based on magnonics. *Appl. Phys. Express* **12**, 070101 (2019).

38. Zhang, W. et al. Generation and transfer of squeezed states in a cavity magnomechanical system by two-tone microwave fields. *Opt. Express* **29**, 11773–11783 (2021).

39. Qian, H., Zuo, X., Fan, Z.-Y., Cheng, J. & Li, J. Strong squeezing of microwave output fields via reservoir-engineered cavity magnomechanics. *Phys. Rev. A* **109**, 013704 (2024).

Acknowledgements

Author contributions

V. A. S. V. B., C. A. P., J. P. D. and A. M. conceived the idea. V.A.S.V.B. and A.M. developed the theory; V.A.S.V.B. wrote the codes used for generating the plots.V. A. S. V. B., C. A. P., J. P. D. and A. M. contributed with scientific discussions, including validation and iterations of the results, and with the manuscript's writing.

Funding

Competing interests

The authors declare no competing interests.

Additional information

Supplementary information The online version contains supplementary material available at https://doi.org/10.1038/s42005-025-02017-0.

Correspondence and requests for materials should be addressed to Victor A. S. V. Bittencourt or A. Metelmann.

Peer review information : *Communications Physics* thanks Myung-Joong Hwang and the other, anonymous, reviewer(s) for their contribution to the peer review of this work.

Reprints and permissions information is available at http://www.nature.com/reprints

Publisher's note Springer Nature remains neutral with regard to jurisdictional claims in published maps and institutional affiliations.